19
Research paper I Оригинални научни рад
DOI 10.7251/STP2215191G
ISSN 2566-4484

Milan Gavrilović, University of Novi Sad, milangavrilovic@uns.ac.rs
Igor Ruskovski, University of Novi Sad, rus_igor@uns.ac.rs
Dubravka Sladić, Faculty of technical sciences, dudab@uns.ac.rs
Aleksandra Radulović, University of Novi Sad, sanjica@uns.ac.rs
Miro Govedarica, University of Novi Sad, miro@uns.ac.rs
Dušan Jovanović, University of Novi Sad, dusanbuk@uns.ac.rs

ANALYSIS AND PREDICTION OF SPATIOTEMPORAL CHANGES OF URBAN AREAS USING NEURAL NETWORKS

Abstract

Land use/Land cover (LULC) is crucial for land management. This study shows the spatiotemporal dynamics of LULC for a wide area of Novi Sad with the emphasis on the urban area analysis. Results presented in this study aim to estimate LULC changes and predict future trends of urban area expansion in Novi Sad. Conducted study shows that in the years to come there will be a decrease in the urban area expansion compared to last 35 years.

Keywords: change detection, LULC, Landsat, neural networks, random forest

АНАЛИЗА И ПРЕДИКЦИЈА ПРОСТОРНО-ВРЕМЕНСКИХ ПРОМЕНА УРБАНОГ ПОДРУЧЈА ПОМОЋУ НЕУРОНСКИХ МРЕЖА

Сажетак

Коришћење земљишта/земљишни покривача (LULC) је од суштинског значаја за управљање земљиштем. Ова студија илуструје просторно-временску динамику LULC ширег подручја Новог Сада, са акцентом на анализу урбаних подручја. Резултати, презентовани у овом раду, имају за циљ да процене промене LULC-а и предвиде будуће трендове ширења урбаног подручја Новог Сада. Проведена студија показује да ће у наредном периоду доћи до споријег ширења урбаног подручја у односу на последњих 35 година.

Кључне ријечи: детекција промена, LULC, Landsat, неуронске мреже, random forests

1. INTRODUCTION

The landscape changes cause various transformations in the nature ecosystems and the structure of society, both physical surroundings and socioeconomic factors. Among these activities, rapid urban development is considered to be leading driver for the loss of arable land and green spaces which can greatly affect climate changes and human life in general [1-3]. Consequently, large-scale urbanization and population growth are causing LULC changes, which could potentially have negative environmental consequences.

Urbanization is a name that denotes the natural or mechanical increase of population in urban areas, the expansion of urban areas or the transformation of predominantly rural characteristics of an area into an urban area. Urbanization is causing rapid land cover change, especially in developing countries [4]. The process of urbanization implies, above all, the development of cities, and in a broader sense, all other human settlements. Urban areas tend to change drastically over a short period [5] of time due to constant urbanization. Urbanization has led to land cover change often in suburban areas as a result of rapid economic development.

Timely and accurate mapping of urban land is necessary to anticipate the resources needed for the normal functioning of the urban area [6]. Remote sensing data are useful for monitoring the spatial distribution and growth of urban areas because of their ability to provide timely and up-to-date data [7]. In the last two decades, researchers have become increasingly interested in using satellite imagery to solve the problem of urban sprawl and suburbs. During this period, numerous techniques were created for fast mapping of both land cover and urban area with the help of satellite images.

In parallel with the development boom of housing, there is also the expansion of institutional, industrial, traffic, infrastructure and other built-up areas. The development of these areas is important for overcoming the problems caused by overcrowding in cities [8].

Change detection represents a serious and challenging task in the field of remote sensing. LULC changes identification based on the satellite image classification is the most common approach for the change detection when it comes to land cover [9]. In order to compare images, pixels from both images have to be compared and this is one of the methods that can answer the question of where and what changes had happened. Multiple studies [10-14] have shown that the changes in LULC, with urban expansion having one with the biggest impact, followed by loss of forests, agricultural land, water bodies, etc., are related to the degradation of the natural environment [1]. Techniques for modeling transition potential and simulating future LULC under the influence of spatial variables have evolved rapidly. They are trying to find out where the change has taken place and where the change will potentially happen in the future [15]. Most of these models take land cover time data in consideration when estimating transition potential, which in combination with spatial variables can predict future LULC scenarios [1,16].

This paper main focus is the analysis of LULC changes in the past 35 years and simulation of the future state for the wider area of Novi Sad. The assumption is that there will be a somewhat slower urbanization and expansion of the city of Novi Sad, since the city area has drastically increased in the last 35 years, and that this trend of expansion will be transferred to greater urbanization of surrounding suburbs. In order to confirm or reject these assumptions, this research is conducted with the main goal to predict changes in land cover using the method of Multilayer Perceptron (MLP) Neural Network. As foretold, the emphasis is on the analysis of urban sprawl in the last 35 years and the simulation of urban sprawl in the next 35 years using publicly available data sets and open source tools.

2. MATERIALS AND METHODOLOGY

2.1. STUDY AREA

The area for this analysis includes the wider urban area of Novi Sad. The city of Novi Sad is located at 45°15′18″N, 19°50′41″E, and is the largest city in the Autonomous Province of Vojvodina. The town lies on the banks of the river Danube, on the left bank is the plain part of the city (Backa), while on the right bank is the hilly part of the city (Srem), located on the slopes of Fruska gora. The altitude on the Backa side is 72-80m, while on the Srem side it is about 250-350m. After Belgrade, Novi Sad is the second most populous city in the Republic of Serbia. At the last official census from 2011., the city itself had 231 798 inhabitants, while in the municipal area of Novi Sad the number of inhabitatns was 341 625 [17]. Novi Sad has a very favorable geographic position, it is located on the important traffic corridors, which provides significant advantages. Its roads, rails and river are

connected to the environment. The city was also chosen as the European Capital of Culture in 2022. and as such it certainly has great potential for expansion.

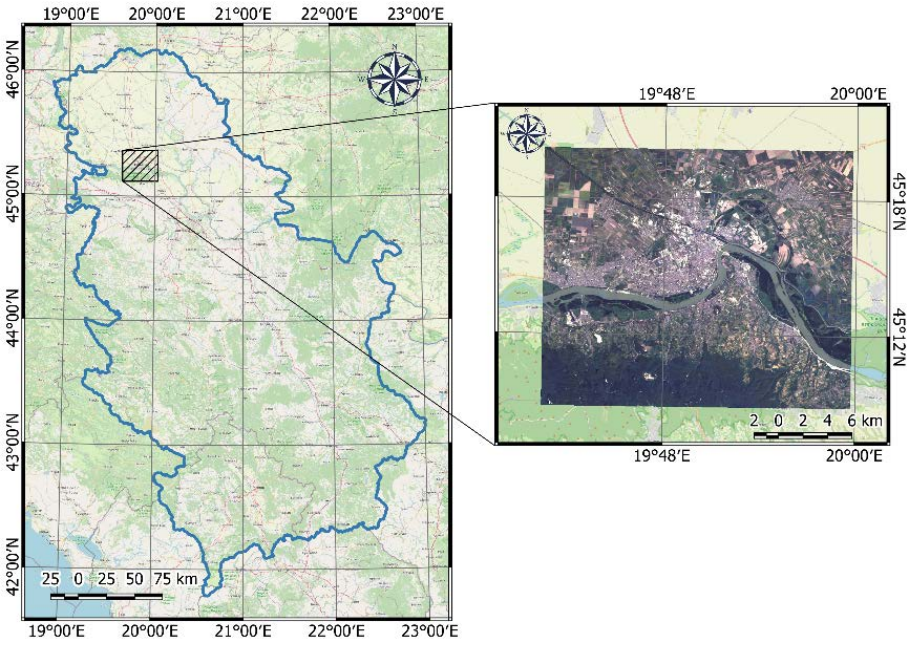

Figure 1. *Study area*

2.2. DATA COLLECTION

The data set for this analysis consisted of satellite images [18] used to obtain land cover maps, digital elevation model and OpenStreetMap data from which other raster data (remoteness from roads and remoteness from watercourses) representing the input parameters of the simulation model were created.

2.2.1. Landsat 5

Landsat 5 was a low-orbit Earth satellite, launched on March 1st, 1984 for the purpose of collecting images of the Earth's surface. It was a continuation of the Landsat program (Landsat 1, 2, 3 and 4 were sent into orbit before Landsat 5). After 29 years spent in space, Landsat 5 completed its mission on June 5th, 2013 [19]. It was equipped with two sensors: Thematic Mapper (TM) and Multispectral Scanner (MSS). Each shot covers an area of 185x170km. The Landsat sensor has 7 bands that simultaneously record the emitted energy from the Earth's surface in blue, green, red, near-infrared, medium-infrared and thermal infrared part of the spectrum, with spatial resolutions of 30m and 120m [20]. The platform was located at an altitude of 705km with an orbit synchronized with the Sun. It had a 16 day temporal resolution.

2.2.2. Landsat 8

Landast 8 was launched on February 11th, 2013. It was fully developed in collaboration between two agencies, the US Geological Survey (USGS) and the National Aeronautics and Space Administration (NASA). Like the Landsat 5, the Landsat 8 also carries two types of sensors, Operational Land Imager (OLI) and the Thermal Infrared Sensor (TIRS). The OLI sensor has a spatial resolution of 30m, while the TIRS thermal sensor has a spatial resolution of 100m. TIRS data are registered together with OLI data that are of higher spatial resolutions to form radiometric and geometric corrections. Landsat 8 records in 11 bands. Of those bands, the tenth and the eleventh are thermal, data from TIRS sensors, the eight band is panchromatic with a spatial resolution of 15m [21]. The Landsat 8 orbit is defined in relation to the Worldwide Reference System (WRS-2) and is synchronized with the Sun and is located at an altitude of 705km. The inclination of the orbit is 98.2 degrees. The satellite orbits the Earth in 98.9 minutes, and the time of crossing the equator is at 10:00 UTC +/- 15 minutes. These characteristics of the orbit allow the Landsat 8 satellite to cover the entire globe every 16 days. The approximate scene covered by one shot is 170x183km [22].

2.2.3. EU-DEM

EU-DEM is a new digital elevation model for Europe. It was developed under the Copernicus program. The aim of the program is to increase the availability and establish the basis for the height of European relief data. The model is of medium quality, with a spatial resolution of about 25m. It

is a hybrid product based on SRTM and ASTER GDEM data combined with mean value measurement approach. EU-DEM was subsequently improved by adding various data. For example, values of heights in areas where there was a large coverage by the clouds were replaced by the data from SRTM model [23]. Statistical validation of EU-DEM v1.0 shows and overall vertical accuracy of 2.9m RMSE. It is consistent with the upgraded version of EU-Hydro, in order to produce a better river network topology [24].

2.3. METHODS

As a part of this case study, the authors proposed a workflow to predict the expansion of the urban area based on data generated on the principles of remote sensing. The proposed steps are shown in Figure 2.

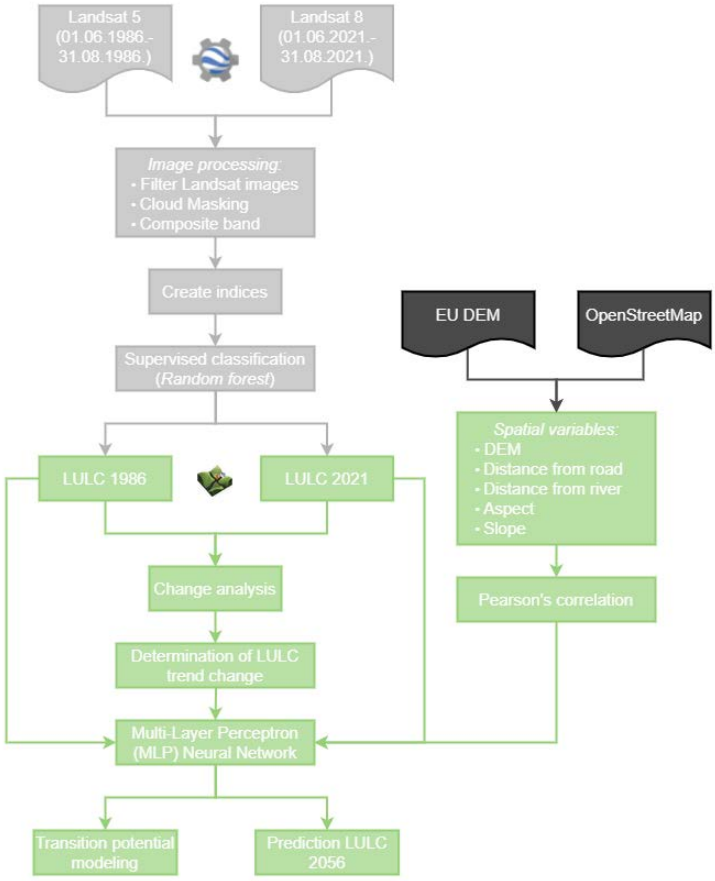

Figure 2. *Flow chart of research method*

2.3.1. Random forest

Random forest is a classifier from the Decision tree classifier group, which produces multiple decision trees using a randomly selected subset of patterns and variables. Random forest is a flexible machine learning (ML) algorithm that is simple, has a very wide application and gives excellent results [25]. This classifier has become popular in the field of remote sensing due to the accuracy of its classifications. It is also one of the most commonly used algorithms, due to its simplicity and the fact that it can be used for both classification and regression, making it similar to SVM. The idea of this algorithm is to train many decision trees and the decision of a class or the unknown sample value is done by voting in the case of classification or averaging the results in the case of regression. Each tree is generated by selecting a random sample from a training set, a pixel with known classes. Attributes that are relevant for classification are selected for tree nodes. In the processing of satellite images relevant attributes are bands. Not all bands are used for individual trees, but some bands are used, ie. the number of tree nodes is less than the number of bands. For each node, based on a known sample, boundary parameters are generated that divide the sample into classes up to the last branch of the decision tree [26]. The procedure is repeated until a sufficient number of trees is generated. Each pixel of the satellite image passes through each tree that classifies it into one of the classes. In the end, the pixel is assigned to the class that a large number of trees have chosen for that pixel.

2.3.2. Change Analysis and Transition Potential Modeling

The Modules for Land-Use Change Simulation (MOULSCE) tool was used in this paper to analyse land cover change and simulate future changes. This QGIS plugin offers the ability to analyse and differentiate land cover change characteristics between two different years. In this study, the change in land cover between 1986 and 2021 was analysed in order to see the changes in spatial patterns. MOULSCE is able to calculate the transition matrix of the probability of change between any given class and generates a map that thematically shows all types of land cover change.

MOLUSCE offers methods such as Artificial Neural Network (Multi-layer Perception), Multi Criteria Evaluation, Weights of Evidence and Logistic Regression for modeling future land cover, ie. simulation of land cover in the coming period. An artificial neural network (ANN) method was used in this study. Cellular Automata Simulation was used to predict future land cover change based on 1986 and 2021 maps and additional spatial variables. What is important to note is that this model is based on the analysis of previous changes in the use and condition of neighboring cells to define the rules of transition, and not on some anthropogenic or natural processes.

2.3.3. Multi-Layer Perceptron (MLP) Neural Network Method

Artificial neural networks represent an alternative approach to solving logical problems compared to conventional computer logic. The very word "artificial" suggests that the inspiration for the structure and logic of these networks came from an attempt to imitate the work of natural neural connections and systems. Basically, the use of artificial neural networks tries to create an artificial system capable of learning and making intelligent decisions as a human being. This is especially important when it comes to the large amount of data and the short time required to process it.

The perceptron is a model of a single neuron that was the forerunner of larger neural networks. For multi-class problems, it is necessary to use more perceptrons, one for each class. The output of each perceptron represents the probability of belonging to that class, and the class with the highest probability is taken as the final output. A neural network is characterized as a Multi-layer perceptron if within the neural network there are additional layers of neurons (perceptrons) between the input and output layers, so-called hidden layers [27,28], as shown in Figure 3. The input layer receives an input signal that should be processed. The required task such as prediction and classification is performed by the output layer. An arbitrary number of hidden layers located between the input and output layers are the real computational mechanism of MLP [27]. MLPs are designed to approximate any continuous function and can solve non-linear problems [28]. MLPs are most commonly used for classification problems, recognition, prediction, and approximations.

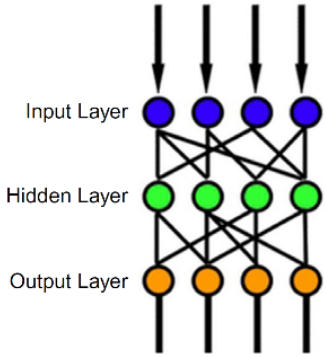

Figure 3. *Schematic representation of a MLP with single hidden layer [28]*

3. RESULTS AND DISCUSSION

3.1. CLASSIFICATION

In order to be able to analyse the change in land cover and the expansion of the urban area, it is necessary to classify satellite images and extract class information from them. Before the classification, a search of satellite images from two collections (Landsat 5 and Landsat 8) for the period from June to September 1986 and 2021 for the wider area of Novi Sad was performed. Clouds were removed from the images obtained in this way, and composites were created in order to obtain one image for 1986 and 2021 (Figure 4). In order to obtain better classification results, and based on the analysis of the literature that dealt with the classification of land cover [29-31], it was decided to add 5 more indices (NDVI, NDWI, NDBI, SAVI and EBBI) in addition to satellite imagery bands.

Figure 4. *RGB satellite image 1986 (a) and 2021 (b)*

Prior to the classification procedure, training samples were made for each of the 5 classes (water, forest, bare land, low vegetation and artificial objects), 400 for each of the two analysed years. Since the data about classes have not been available, training samples were created through the satellite images analysis. In order to claim with certainty that those pixels that represent areas of a certain class are included, optical images are visually displayed with different combinations of RGB displays of visible and infrared bands. Out of the total number of training samples, 80% were taken for training and 20% were taken for accuracy assesment.

The classification of satellite images was performed using the already implemented Random Forest algorithm within Google Earth Engine. Satisfactory classification results were obtained by minimal modification of parameters, so the number of trees for each class (numberOfTrees) was chosen to be 300, and the input of tree variables (bagFraction) was chosen to be 0.5, other parameters were left at default values. In the paper itself, as already mentioned, the emphasis is placed on the analysis of changes in land cover, ie. on the analysis of the expansion of the urban area, and for that reason no greater attention was paid to the optimization of the parameters of the classification algorithm.

The results of the satellite image classification were confirmed by estimating pixel-by-pixel accuracy based on validation points. Validation points were selected at different locations representing different land cover classes. For each classification result, an accuracy check was performed based on the error matrix and Kappa statistics of the same. An overall classification accuracy of 93.51% for 1986 and 94.59% for 2021, respectively, was obtained, with Kappa statistics of 91.79% for 1986 and 92.80% for 2021.

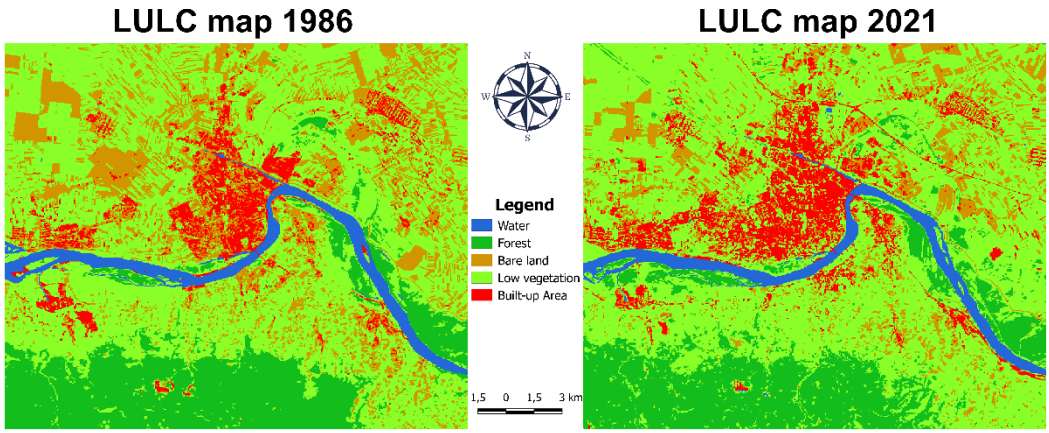

Figure 5. *LULC maps 1986 and 2021*

3.2. LULC CHANGE ANALYSIS

After the classification, the analysis of the change in the way of land cover in the last 35 years was performed, ie. for the period from 1986 to 2021. LULC maps classified into five LULC classes are shown in Figure 5. What can be seen from these maps is that the area occupied by artifical objects has increased significantly in the last 35 years. This increase in artificial areas is most noticeable on the western side of the city of Novi Sad, which in terms of construction resulted in the merger of

Novi Sad with the suburban settlement of Futog. The spread of other suburban settlements is also visible.

Table 1 shows the areas of each of the five analysed land cover classes, as well as their differences. It is obvious that the biggest change was experienced by bare land, which partly passed into the class of built-up areas, and partly into the class of low vegetation. Given that the classes of low vegetation and bare land can represent arable land, it is clear that the change in the way of use between these two classes will occur not only from year to year but also within one year. What can be concluded from this table is that there was a small change in water surfaces (decrease in area of 0.18%) and a slight increase in forest area of 1.28km^2 and 0.25%. On the other hand, the use of urban land has increased significantly by 19.83km^2.

Table 1. Class statistics

LULC Type	1986 [km^2]	2021 [km^2]	D [km^2]	D [%]
Water	20.20	19.29	-0.91	-0.18
Forest	86.29	87.57	1.28	0.25
Bare land	103.22	60.02	-43.20	-8.44
Low vegetation	270.57	293.57	23.00	4.49
Built-up Area	31.80	51.62	19.83	3.87

Analysis of LULC changes shows a proportional transformation of bare soil into vegetation classes and artificial objects (Figure 6). Based on the share of representation of each class, it can be clearly established that new urban areas have emerged on parts of once potentially arable land (low vegetation and bare land).

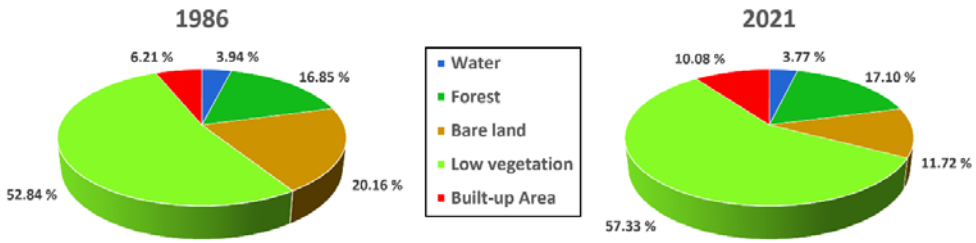

Figure 6. *Different composition of land cover percentage in 1986 and 2021*

Figure 7 shows the areas that now belong to the artificial objects and which in 1986 belonged to one of the other four classes. From this picture, it is noticeable that most areas where there was no vegetation were transformed into artificial surfaces. More precisely, as much as 56.17% of the total number of transformed areas on which there was bare land was transformed into artificial objects, and the rest of the area of 43.83% was transformed into other 3 classes.

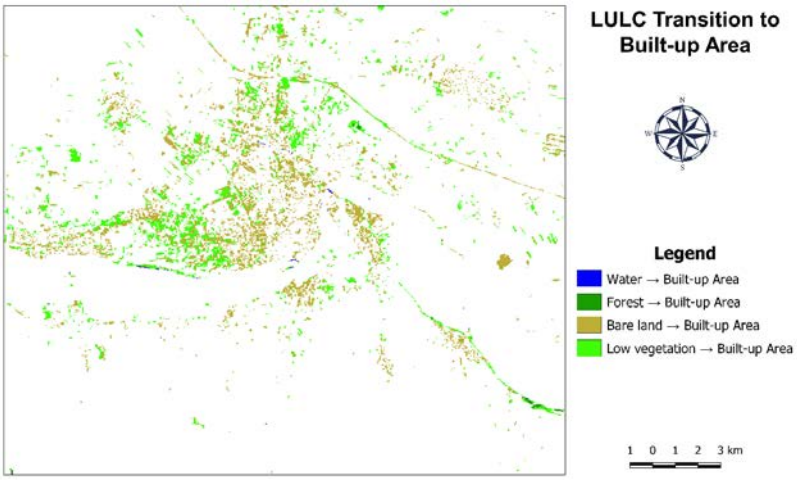

Figure 7. *LULC Transition to Built-up Area*

The percentage of all classes that were transformed into artificial surfaces is given in Figure 8. As already mentioned, bare land experienced the biggest change, and now it can be seen that the smallest change occurred in water surfaces, which was expected.

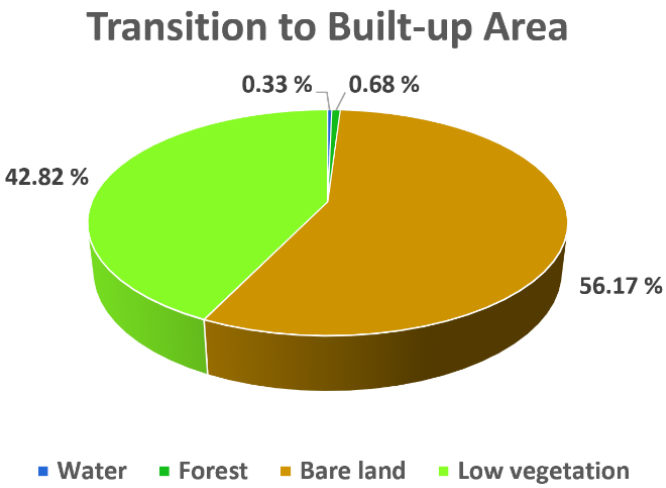

Figure 8. *Percentage Transition to Built-up Area*

3.3. CORRELATION EVALUATION

In order to more accurately predict the further expansion of the urban area in addition to the land cover from the two periods (maps obtained in the previous step), it is necessary to include other data that may affect the forecast result in the analysis. More precisely, the result of the forecast can be influenced by some physical and socioeconomic factors that are responsible for changes in LULC, because their contribution to the mechanism of change is very significant. Spatial factors such as the digital elevation model, aspect, slope, distance from roads and distance from watercourses can greatly influence the expansion of the urban area, so they are included in the model based on which predictions of the situation for the next 35 years will be made.

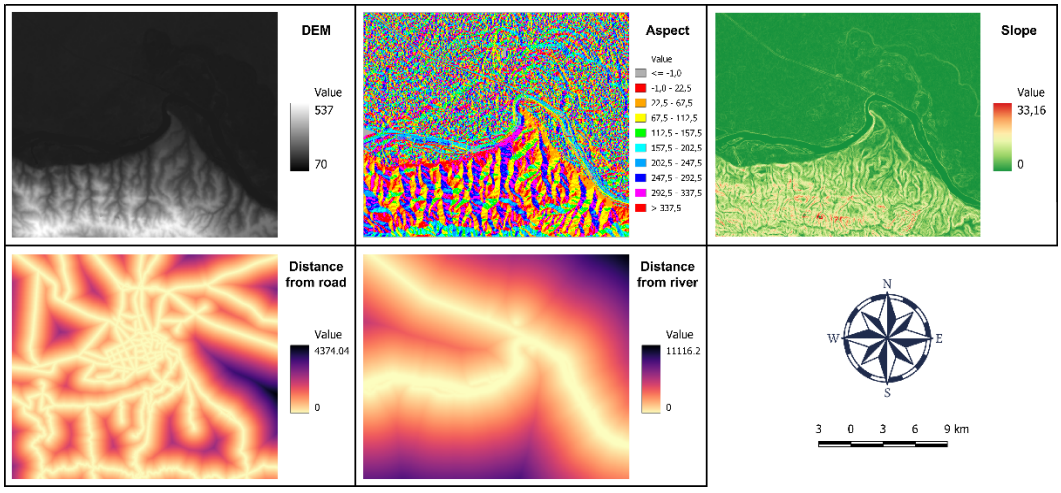

Figure 9. *Spatial variables*

The correlation between the spatial variables was estimated using Pearson's correlation coefficient. The correlation coefficient takes values from -1 to +1. If it takes positive values, the correlation between the phenomena is direct or positive (both phenomena show direct variations). In the case when the correlation coefficient is less than 0, the relationship is inverse or negative (when one phenomenon increases, the other decreases, and vice versa). If there is a functional connection between the observed phenomena, we are talking about a perfect correlation. The correlation coefficient in that case takes the value -1 (if the connection is inverse) or +1 (if the connection is direct). The closer the absolute correlation coefficient is to value of one, the stronger the correlation between the phenomena. In contrast, the closer to zero the weaker the linear relationship. Table 2 shows the correlation relationship between the five spatial variables. As we can see, DEM and Slope have the greatest dependence, and DEM and Aspect have the least.

Table 2. Person's correlation between spatial variables

	DEM	Aspect	Distance from road	Slope	Distance from river
DEM	--	-0.00624	-0.07703	0.75050	0.51109
Aspect		--	-0.01326	-0.01012	0.01274
Distance from road			--	-0.05230	0.06236
Slope				--	0.30852
Distance from river					--

3.4. TRANSITIONAL POTENTIAL MODELING

Based on LULC data and spatial variables, a transition probability matrix is formed, which consists of rows and columns of land classes in the initial 1986 and final 2021 year. This matrix shows the proportion of pixels that change from one type to another.

The highest probability of change of 0.176696 was observed when changing bare land into built-up land, which coincides with previous analyses. The lowest probability of change is when crossing water surfaces into bare land and it is zero, which tells us that this kind of transformation will not happen.

Table 3. Transition matrix of land cover in 1986 and 2021

		2021				
		Water	**Forest**	**Bare land**	**Low vegetation**	**Built-up Area**
1986	**Water**	0.888027	0.011139	0	0.095531	0.005302
	Forest	0.002076	0.823856	0.001439	0.170084	0.002545
	Bare land	0.002842	0.008405	0.209776	0.602281	0.176696
	Low vegetation	0.001956	0.056348	0.124448	0.765856	0.051392
	Built-up Area	0.011095	0.004359	0.143836	0.238367	0.602343

Once the transition matrix has been formed, the next step is to create a model to predict land cover change. During the process of model creation, LULC data from years 1986. and 2021. was used as an input, along with spatial variables and transition matrix (Table 3) in order to predict the LULC for the year of 2056.In this paper, the Multi-Layer Perceptron (MLP) neural network algorithm was used to simulate the future state, as literature analysis found that many researchers found that this approach was more powerful than other methods such as linear regression [32,33]. When creating a model, it is necessary to define several parameters, so the value of one pixel was chosen for Neighborhood pixels because it is the minimum that is the most efficient. Ten hidden layers were selected, the learning rate and momentum parameters were set to 0.001, and the training was performed in fify iterations. After this, it was determined that the total accuracy is -0.00082, and the Min Validation Overall Error is 0.06328. In the following diagram, we see the learning curve of the model, which is obtained in the process of training the neural network.

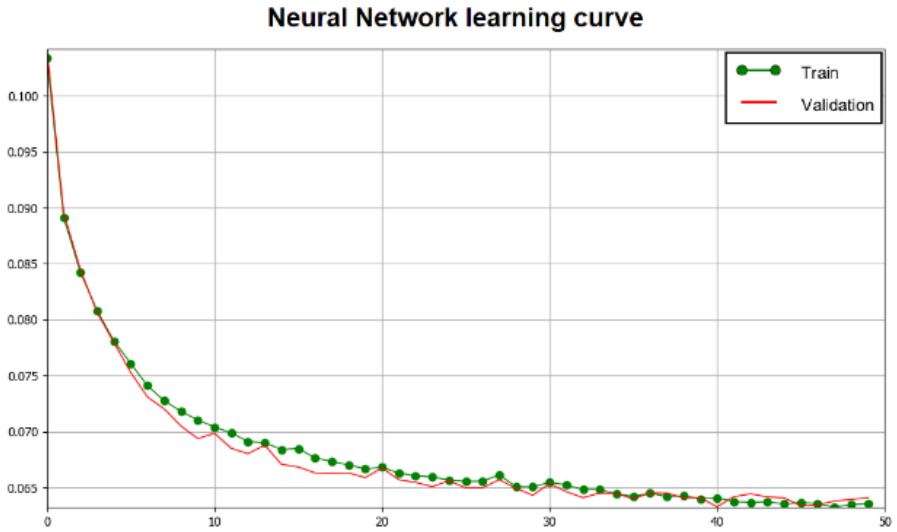

Figure 10. *Neural Network learning curve*

3.5. PREDICTION LULC

In this case, artificial neural network was used to model the transition potential, and the results generated in this way will be used in the further process, ie. in Cellular Automata Simulation. Basically, the Cellular Automata Simulation process is based on the Monte Carlo algorithm [1,10]. Future LULC maps are predicted assuming that the existing LULC pattern and dynamics continue. The simulation results are shown in the following maps. Since low vegetation and bare land have the greatest potential for change into built land, only these two types will be shown below, the other two types (water and forest) show less than 10% of the potential to move to urban areas, so they will not be further analysed.

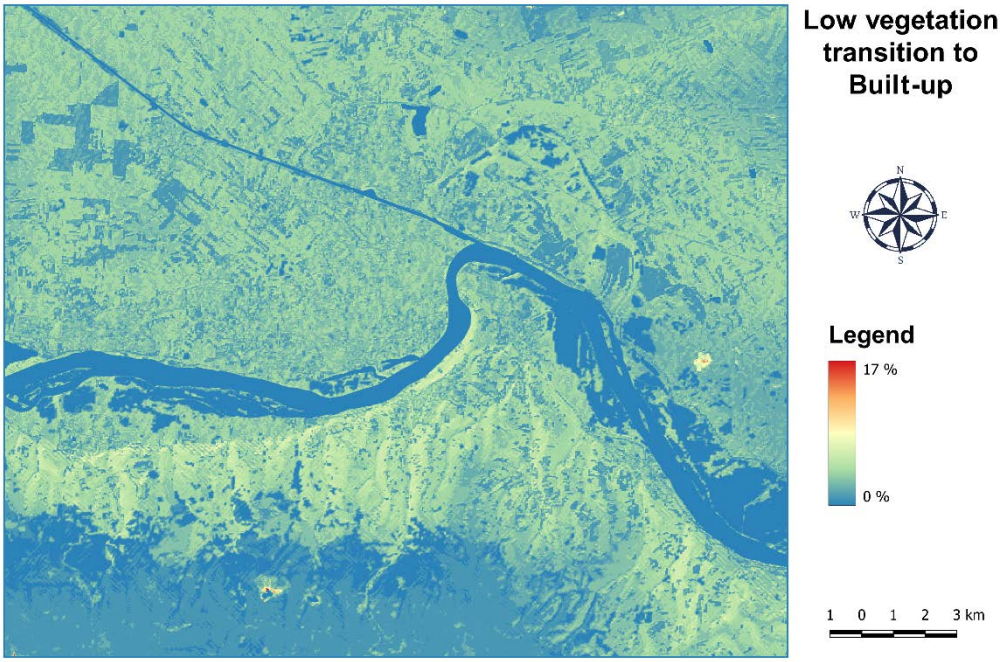

Figure 11. *Low vegetation transition to Built-up*

As Figure 11 shows, low vegetation has the same potential for change in urban areas throughout, but this potential is still below 20%, suggesting a low probability of transition from this class of land to built-up area.

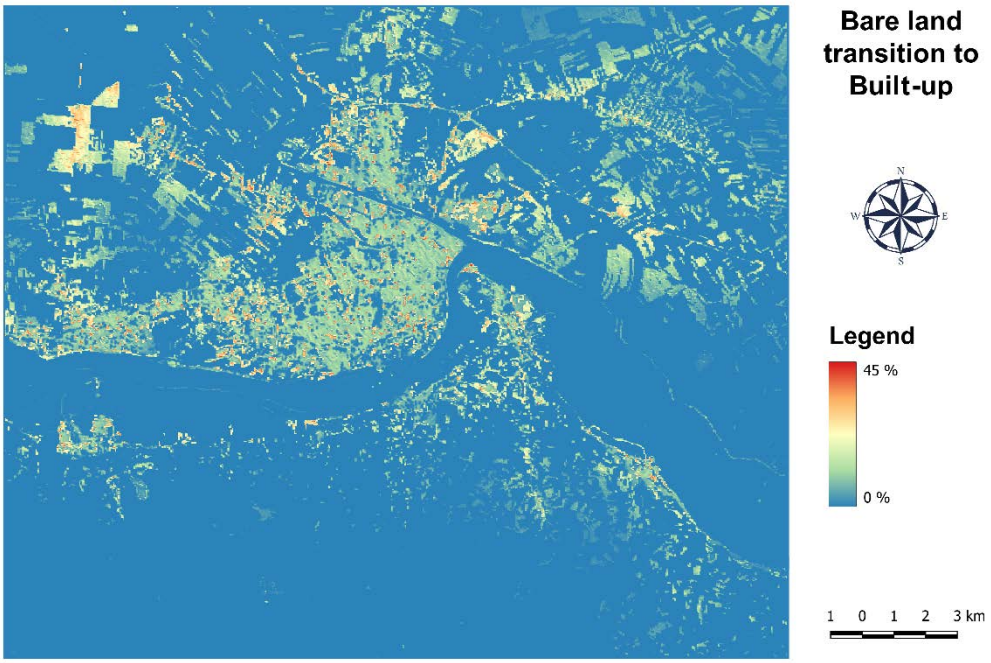

Figure 12. *Bare land transition to Built-up*

On the other hand (Figure 12), with bare land there is a greater potential for change, up to 45%, which indicates a higher probability of transition of this type of land to built-up, so it is quite realistic to expect a transition in this direction. The result of the simulation and the ultimate goal of this analysis is a map of the projected spatial distribution of artificial objects for 2056.

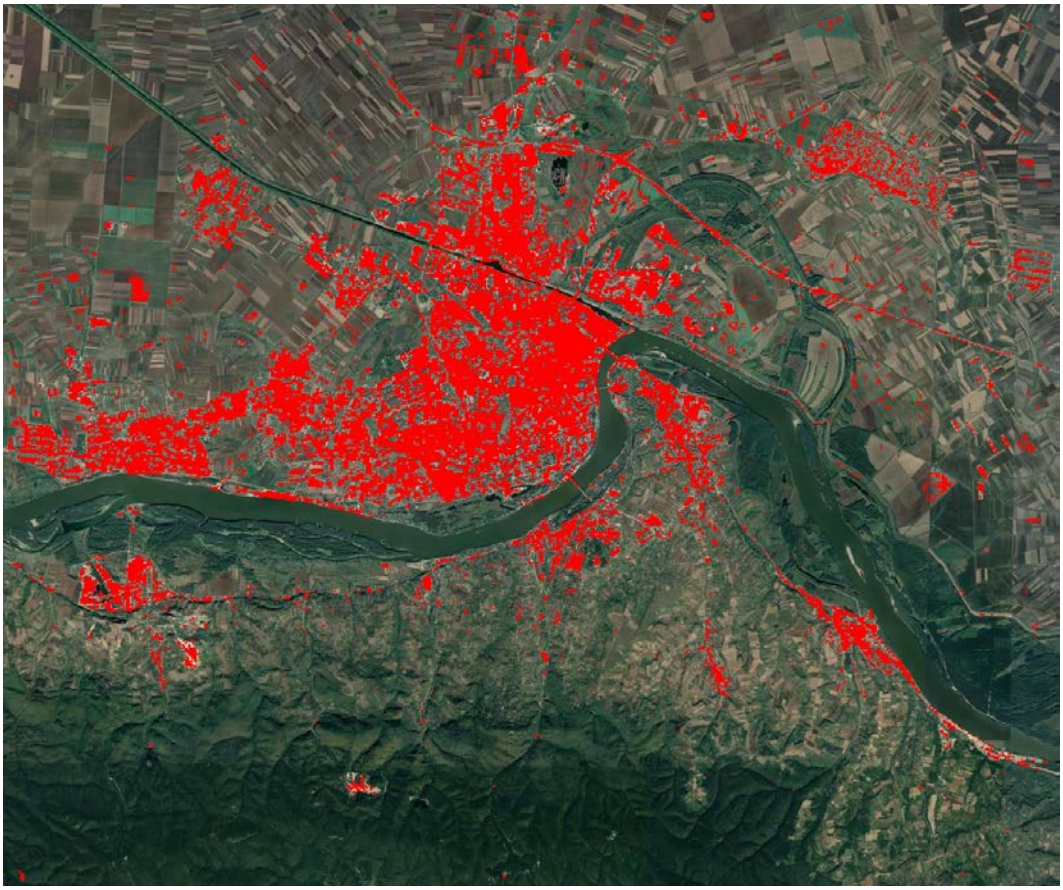

Figure 13. *Built-up area in 2056*

As it can be seen from Figure 13, in the next 35 years, slow urbanization is predicted, ie. the trend of urban expansion is weakening. Based on the calculated areas for each class, we can see that the share of artificial facilities for 2056 in the wider area of Novi Sad is 10.82%, which confirms the previous conclusion about a small increase in the urban area. This conclusion makes sense if we take into account the fact that the city has experienced a drastic expansion in the last 35 years, which has been proven in this paper, so it is to be expected that further expansion will be somewhat slower. In addition to the expansion of the city of Novi Sad, there is also a change in the area, ie. expansion of surrounding settlements.

4. CONCLUSION

LULC maps from 1986 and 2021 represent a significant source of data and as such were used to simulate changes in 2056. The results of the classification indicate a significant growth of the urban area during the analysed period, with a decrease in other types of land cover.

The results of this research show that the greatest transformation into built land, in the last 35 years, of all LULCs, has been experienced by areas under low vegetation and bare land. Specifically, the LULC class, which experienced the largest change in the decrease from 1986 to 2021, was the bare land class, which was determined to have passed most of these areas into the class of built-up areas. During the analysis of areas and representation of each class in the analysed area, it was determined that the construction area of the wider area of Novi Sad in 1986 was 31.8km^2, and the construction area in 2021 was 51.62km^2. Further analysis concludes that the area of Novi Sad has expanded by 19.83km^2 over 35 years. The biggest changes and urban expansion have been identified in the area of Veternik and Telep.

Spatial variables, such as Digital elevation model, Slope, Aspect and Distance and Road Distance Factors, are very important driving factors that determine the further transformation of LULC, and as such are recognized and included in the model used to simulate future conditions . The use of the Multi-Layer Perceptron (MLP) as a model to simulate the future state of LULC for 2056 using Cellular Automata Simulation has shown that the areas under artificial objects are slightly increasing compared to 2021. This result confirms the initial assumption that in the coming period there will be a slow expansion of the urban area. Additional improvements to the proposed model could be achieved by including more spatial variables that influence the change of landscape patterns, so the analysis of other physical and socio-economic factors that may be responsible for land cover change will be the subject of future research.

This study proposed a model for simulating the future expansion of the urban area, which can be of great help for planning the development of cities, ie. to create settlement regulation plans or to solve problems that arise due to various human activities. Also, the results obtained in this way can be used by planners to determine a development pattern that would allow them to make better use of land. In addition, it helps the community understand the changes in its environment, as well as other stakeholders to assess the development potential of a place. It also provides vital information to state or local authorities that are directly involved in the development of an area. By analyzing future potential developments, using publicly available data and open source tools, data obtained can be used by experts from various fields that are in some way related to spatial and temporal data.

ACKNOWLEDGMENTS

This work was financially supported by the Ministry of Education, Science and Technological Development of the Republic of Serbia Grants No. 37017.

LITERATURE

[1] Z. Abbas, G. Yang, Y. Zhong, and Y. Zhao, “Spatiotemporal Change Analysis and Future Scenario of LULC Using the CA-ANN Approach: A Case Study of the Greater Bay Area, China,” *Land*, vol. 10, no. 6, pp. 584, 2021.

[2] R. Wang, A. Derdouri, and Y. Murayama, “Spatiotemporal Simulation of Future Land Use/Cover Change Scenarios in the Tokyo Metropolitan Area,” *Sustainability*, vol. 10, no. 6, pp. 2056, 2018.

[3] Z. Qiao, L. Liu, Y. Qin, X. Xu, B. Wang, and Z. Liu, “The Impact of Urban Renewal on Land Surface Temperature Changes: A Case Study in the Main City of Guangzhou, China,” *Remote Sensing*, vol. 12, no. 5, pp. 794, 2020.

[4] L. Jiang, Y. Liu, S. Wu, and C. Yang, "Study on Urban Spatial Pattern Based on DMSP/OLS and NPP/VIIRS in Democratic People's Republic of Korea," *Remote Sensing*, vol. 13, no. 23, pp. 4879, 2021.
[5] Z. Wu, R. Zhou, and Z. Zeng, "Identifying and Mapping the Responses of Ecosystem Services to Land Use Change in Rapidly Urbanizing Regions: A Case Study in Foshan City, China," *Remote Sensing*, vol. 13, no. 21, pp. 4374, 2021.
[6] S. Gao, W. Li, K. Sun, J. Wei, Y. Chen, and X. Wang, "Built-Up Area Change Detection Using Multi-Task Network with Object-Level Refinement," *Remote Sensing*, vol. 14, no. 4, pp. 957, 2022.
[7] D. Jovanović, M. Gavrilović, D. Sladić, A. Radulović, and M. Govedarica, "Building Change Detection Method to Support Register of Identified Changes on Buildings," *Remote Sensing*, vol. 13, no. 16, pp. 3150, 2021.
[8] C. Corbane, V. Syrris, F. Sabo, P. Politis, M. Melchiorri, M. Pesaresi, P. Soille and T. Kemper, "Convolutional neural networks for global human settlements mapping from Sentinel-2 satellite imagery," *Neural Computing and Applications*, vol. 33, pp. 6697, 2021.
[9] D. Jovanović, M. Govedarica, F. Sabo, Ž. Bugarinović, O. Novović, T. Beker and M. Lauter, "Land cover change detection by using remote sensing: A case study of Zlatibor (Serbia)," *Geographica Pannonica*, vol. 19, no. 4, pp. 162, 2015.
[10] N. Alam, S. Saha, S. Gupta, and S. Chakraborty, "Prediction modelling of riverine landscape dynamics in the context of sustainable management of floodplain: a Geospatial approach," *Annals of GIS*, vol. 27, no. 3, pp. 299, 2021.
[11] C. Liping, S. Yujun and S. Saeed, "Monitoring and predicting land use and land cover changes using remote sensing and GIS techniques—A case study of a hilly area, Jiangle, China," *PLOS ONE* vol. 13, no. 7, 2018.
[12] C. Başnou, E. Álvarez, G. Bagaria, M. Guardiola, R. Isern, P. Vicente and J. Pino, "Spatial Patterns of Land Use Changes Across a Mediterranean Metropolitan Landscape: Implications for Biodiversity Management," *Environmental Management*, vol. 52, pp. 971, 2013.
[13] X. Jianchu, J. Fox, J. B. Vogler, Z. P. F. Yongshou, Y. Lixin, Q. Jie and S. Leisz, "Land-Use and Land-Cover Change and Farmer Vulnerability in Xishuangbanna Prefecture in Southwestern China," *Environmental Management*, vol. 36, pp. 404, 2005.
[14] N. Gamboa-Badilla, A. Segura, G. Bagaria, C. Basnou and J. Pino, "Contrasting time-scale effects of land-use legacy on species richness, diversity and composition in Mediterranean scrubland communities," *Landscape Ecology*, vol. 35, pp. 2745 ,2020.
[15] S. W. Wang, B. M. Gebru, M. Lamchin, R. B. Kayastha, and W. K. Lee, "Land Use and Land Cover Change Detection and Prediction in the Kathmandu District of Nepal Using Remote Sensing and GIS," *Sustainability*, vol. 12, no. 9, pp. 3925, 2020.
[16] M. Kamaraj and S. Rangarajan, "Predicting the Future Land Use and Land Cover Changes for Bhavani Basin, Tamil Nadu, India Using QGIS MOLUSCE Plugin," *Environmental Science and Pollution Research*, 2022.
[17] Statistical Office of the Republic of Serbia, https://www.stat.gov.rs/en-US/, [12.02.2022.].
[18] D. Jovanović, M. Govedarica, F. Sabo and D. Sladić, "Open Satellite Data for the area of Serbia," in *ICIST 2015 5th International Conference on Information Society and Technology*, 2015.
[19] Landsat 5, https://www.usgs.gov/landsat-missions/landsat-5, [15.02.2022.].
[20] A. Sekertekin and S. Bonafoni, "Land Surface Temperature Retrieval from Landsat 5, 7, and 8 over Rural Areas: Assessment of Different Retrieval Algorithms and Emissivity Models and Toolbox Implementation," *Remote Sensing*, vol. 12, no. 2, pp. 294, 2020.
[21] Landsat 8, https://landsat.gsfc.nasa.gov/satellites/landsat-8/, [15.02.2022.].
[22] M. A. Ridwan, N. A. M. Radzi, W. S. H. M. W. Ahmad, I. S. Mustafa, N. M. Din, Y. E. Jalil, A. M. Isa, N. S. Othman and W. M. D. W. Zaki, "Applications of Landsat-8 Data: a Survey," *International Journal of Engineering & Technology*, vol. 7, no. 4, pp. 436, 2018.
[23] A. Šiljeg, M. Barda, I. Marić, *Digitalno modeliranje reljefa*. Sveučilište u Zadru, Alfa d.d., Zadar, Zagreb, 2018.
[24] EU-DEM, https://land.copernicus.eu/imagery-in-situ/eu-dem, [17.02.2022.].
[25] M. Belgiu and L. Drăguţ, "Random forest in remote sensing: A review of applications and future directions," *ISPRS Journal of Photogrammetry and Remote Sensing*, vol. 114, pp. 24, 2016.

[26] G. Jakovljević, D. Sekulović and M. Govedarica, "Land use / land cover mapping from sentinel 2 data using machine learning algorithms," in *STEPGRAD International scientific conference on contemporary theory and practice in construction XIII*, pp. 247, 2018.
[27] F. Murtagh, "Multilayer perceptrons for classification and regression," *Neurocomputing*, vol. 2, no. 5–6, pp. 193, 1991.
[28] S. Abirami and P. Chitra, "Chapter Fourteen - Energy-efficient edge based real-time healthcare support system," *Advances in Computers, Elsevier*, vol. 117, no. 1, pp. 339, 2020.
[29] Abd. R. As-syakur, I. W. S. Adnyana, I. W. Arthana, and I. W. Nuarsa, "Enhanced Built-Up and Bareness Index (EBBI) for Mapping Built-Up and Bare Land in an Urban Area," *Remote Sensing*, vol. 4, no. 10, pp. 2957, 2012.
[30] A. Taufik and S. S. S. Ahmad, "Land cover classification of Landsat 8 satellite data based on Fuzzy Logic approach," in *8th IGRSM International Conference and Exhibition on Remote Sensing & GIS*, 2018.
[31] M. Ukhnaa, X. Huo and G. Gaudel, "Modification of urban built-up area extraction method based on the thematic index-derived bands," in *IOP Conference Series Earth and Environmental Science 227*, 2019.
[32] M.T.U. Rahman, F. Tabassum, M. Rasheduzzaman, H. Saba, L. Sarkar, J. Ferdous, S.Z. Uddin and A.Z. Islam, "Temporal dynamics of land use/land cover change and its prediction using CA-ANN model for southwestern coastal Bangladesh," *Environmental Monitoring and Assessment*, vol. 189, 2017.
[33] A.M. El-Tantawi, A. Bao, C. Chang and Y. Liu, "Monitoring and predicting land use/cover changes in the Aksu-Tarim River Basin, Xinjiang-China (1990–2030)," *Environmental Monitoring and Assessment*, vol. 191, 2019.